[10]J. F. Janni, Air Force Weapons Laboratory Report No. AFWL-TR-65-150, 1966 (unpublished).
[11]S. W. Robinson and R. D. Bent, Phys. Rev. 168, 1266 (1968).
[12]L. F. Chase, Jr., R. G. Johnson, F. J. Vaughn, and E. K. Warburton, Phys. Rev. 127, 859 (1962).
[13]Chromium Corporation of America, Grade C (light tight, with a thickness variation of ±20%).
[14]M. J. Throop, G. C. Morrison, and D. H. Youngblood, Bull. Am. Phys. Soc. 13, 606 (1968).
[15]D. Kurath, private communication.
[16]E. K. Warburton, J. W. Olness, S. D. Bloom, and A. R. Poletti, Phys. Rev. 171, 1178 (1968).
[17]F. C. Barker, private communication quoted in Ref. 2.

PHYSICAL REVIEW C VOLUME 3, NUMBER 2 FEBRUARY 1971

Survey of (p, t) Reactions in the $1p$ Shell*

S. Kahana
Brookhaven National Laboratory, Upton, New York 11973
and
D. Kurath†
State University of New York, Stony Brook, New York 11790
(Received 5 November 1970)

A comprehensive survey of 21 (p,t) reactions for a wide range of $1p$-shell nuclei is made using zero-range distorted-wave Born-approximation codes and previously calculated two-particle fractional parentage coefficients. Average optical parameters are used for the proton and triton potentials in an attempt to relate magnitudes of transitions in different nuclei. A reasonable fit is obtained to the experimental data, but there remain discrepancies in strong transitions for target nuclei with $A \geq 14$. An effect of $(2s\text{-}1d)$ admixture which acts differently in $L=0$ and $L=2$ transfer is proposed as a likely explanation of this difficulty.

I. INTRODUCTION

In principle, the two-nucleon-transfer reaction is a sensitive probe of nuclear structure. In practice it is also a sensitive probe of the nuclear-reaction theory. Most properties of the nuclei between He^4 and O^{16} are well described in terms of $1p$ configurations for the nuclear wave functions. A study[1] of the (d, p) reaction in this region has shown that the extracted spectroscopic information is in good agreement with calculated $1p$ values if average parameters are used in the optical-model calculations. It seemed worthwhile to us to perform a survey of the two-particle transitions in the same spirit. Cohen and Kurath[2] have published the structural ingredients of such a survey, the two-particle fractional parentage coefficients (c.f.p.'s).

A large number of two-particle-transfer reactions have been measured in the $1p$ region. Most experiments have been interpreted using some form of distorted-wave Born-approximation (DWBA) analysis. However, differential optical potentials are used in the analyses, and often only the shape of the angular distribution (and hence the transferred L value) is determined. Certainly no attempt has been made to relate magnitudes of cross sections for states in different nuclei. The possibility least fraught with complication is presented by 20 (p, t) transitions with incident proton energy between 40 and 50 MeV and target mass number A between 10 and 16. In analyzing these transitions we have made extensive use of the zero-range DWBA codes TWO PAR and DWUCK, and are grateful to their respective authors, B. F. Bayman and P. D. Kunz, for their kind cooperation.

Our first concern is to see how well one can represent the observed angular distributions and magnitudes of the cross sections with an average optical potential containing a single normalization parameter. Secondly, there is the possibility of investigating the spectra of isobaric analog states for which structure calculations often give large amplitudes and distinctive state-dependent variation. Finally, should first-order agreement with experiment be obtained, it may prove possible to look for small admixtures of $(2s\text{-}1d)$ components in the nuclear wave functions.

Section II is devoted to a comparison of experiment with calculations based on the $1p$ shell model and to some comments on the results of this comparison. Section III contains a discussion divided between a brief consideration of the validity of the DWBA analysis and a calculation of the effects of $(2s\text{-}1d)$ admixtures.

II. COMPARISON WITH EXPERIMENT

In Table I we list the experimental (p,t) cases[3-11] used in our comparison together with Q values and possible values of orbital angular momentum transfer L. It is generally assumed in a DWBA analysis that the optical potentials are determined from elastic data in the entrance and exit channels. These potentials are then usually state and energy dependent. We intend, however, to use average proton and triton potentials throughout. This procedure is reasonably justified for the proton; the proton energies are restricted to the range 40–50 MeV in the experiments analyzed. The final-state tritons possess lab energies varying between 13 and 40 MeV, and there are few elastic scattering data[12] available for this projectile. Accordingly, two approaches have been adopted to determine the triton optical potential: (a) to vary the optical parameters within reasonable limits so as to obtain a good fit to the transitions in a particular target nucleus N^{15}; (b) to choose a potential which more or less fits the known elastic data. The resultant potentials[13] S and V differ significantly only in their imaginary components, S containing only surface absorption and V only volume absorption. The optical parameters are listed in Table II and in Fig. 1 is shown a comparative fit to the triton elastic scattering data[12] at 20 MeV in C^{12}.

TABLE I. Experimental data for the transitions $Z^A(p,t)Z^{A-2}$. The first column gives the target nucleus and the (J,T) of the final state. The second, third, and fourth columns give the lab proton energy, transferred orbital angular momentum L, and the Q values, respectively. The fifth column contains the integrated cross section from c.m. angle 15 to 50° except in the case of B^{11} where the limits are 20 to 55°. The final column is a list of the experimental references.

Target→	(IT)	E_{proton} (MeV)	L	$-Q$ (MeV)	$\int_{15}^{50} d\sigma$ (μb)	Reference
O^{16}→	0 1	43.7	0	20.41	705	3
N^{15}→	$\frac{1}{2}$ $\frac{1}{2}$	43.7	0	12.91	699	4
	$\frac{3}{2}$ $\frac{1}{2}$		2	16.42	385	
	$\frac{5}{2}$ $\frac{1}{2}$		2	20.29	629	
	$\frac{3}{2}$ $\frac{3}{2}$		2	27.98	53	
N^{14}→	1 1	43.7	0,2	22.14	201	5
	2 1		2	23.11	118	
C^{14}→	0 0	39.8	0	4.64	768	6
	2 0		2	9.08	1362	
C^{13}→	$\frac{3}{2}$ $\frac{1}{2}$	49.6	2	15.18	988	7
	$\frac{1}{2}$ $\frac{1}{2}$		0	17.18	228	
	$\frac{5}{2}$ $\frac{1}{2}$		2	19.48	280	
	$\frac{1}{2}$ $\frac{3}{2}$		0	27.63	170	8
C^{12}→	0 1	50.0	0	23.32	971	9
	2 1		2	26.68	397	
B^{11}→	$\frac{3}{2}$ $\frac{1}{2}$	43.7	0,2	11.41	805	10
	$\frac{5}{2}$ $\frac{1}{2}$		2	13.74	371	
	$\frac{3}{2}$ $\frac{3}{2}$		0,2	26.08	180	
B^{10}→	2 1	50.0	2	18.53	117	11
	3 1		0,2	20.82	255	

It with surface absorption leads to better fits to the shapes for the targets with $A=14$, 15, and 16. The potential with volume absorption gives better fits to the shapes of the $L=0$ transfer at lower mass number. However, neither gives a better over-all picture of the (p,t) data. Since we have not made any attempt to obtain the best potentials by searches on the parameters, no special significance should be attached to the values of Table II.

Electron scattering analyses indicate the rms radii of $1p$-shell nuclei we consider are nearly constant. This suggests that the radii used in the optical wells and in the neutron bound-state well be kept constant, i.e., that no $A^{1/3}$ dependence be included. The fits obtained seem to corroborate this point, although as one might expect the effect is stronger when surface absorption is used for the triton.

The reaction $N^{15}(p,t)N^{13}$ was selected for determining potential S. Of particular interest is the large spread of energies between the four final states in N^{13}, a gap of 15 MeV existing between the $T=\frac{1}{2}$ ground state and the $T=\frac{3}{2}$ analog state. In the shell model one, of course, uses identical single-particle wave functions to construct both states. The two-neutron form factor for the (p,t) reaction must, however, take into account the large difference in separation energy between these states. A complete and easily usable theory of the

TABLE II. The optical parameters for both proton and triton. The so-called constant radius used in this work was obtained by setting $A=15$ in all relations $R_x = r_x A^{1/3}$. Here $V(r) = -Vf_V(r) - iWf_W(r) + 4ia_W W_S f_W'(r)$, with $f_x(r) = (1+e^{(r-r_x A^{1/3})/a_x})^{-1}$.

Particle	V	W	W_S	r_V	r_W	a_V	a_W
Proton	50	5	8	1.20	1.20	0.60	0.60
Triton (surf)	160	0	30	1.20	1.40	0.80	0.80
Triton (vol)	177	20	0	1.14	1.60	0.72	0.77

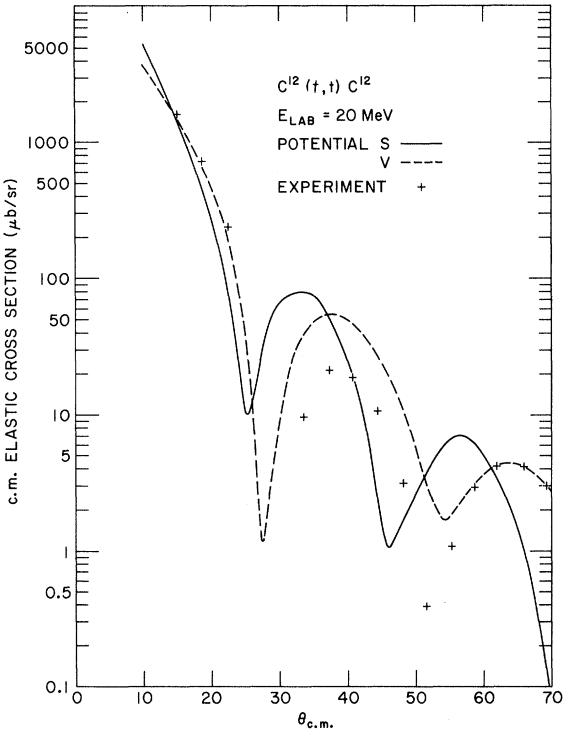

FIG. 1. A comparison with experiment of the triton elastic scattering from the surface absorption potential S and the volume absorption potential V. The experimental data is for a C^{12} target and tritons of lab energy 20 MeV.

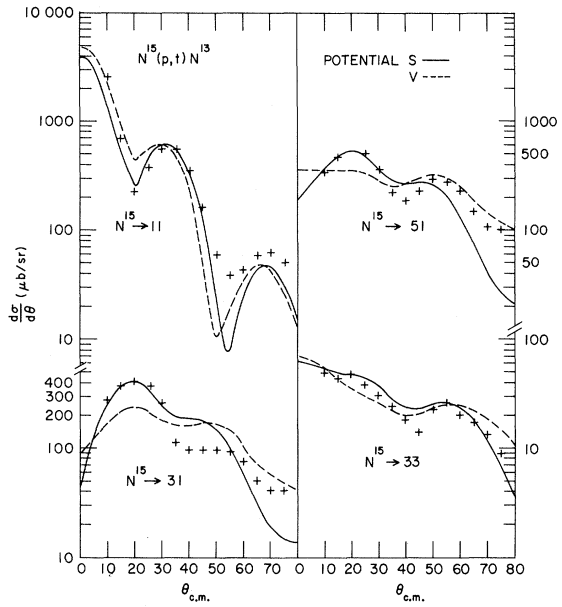

FIG. 2. A comparison with experiment for the angular distributions obtained in the transition from the N^{15} ground state to four states in N^{13}. Here, as in all further angular distributions, the calculated shapes are normalized to the experimental in the neighborhood of the first peak for $L=2$ transfer and the second peak for $L=0$ transfer. The experimental points appear as crosses whose size is in no way an indication of errors. Final-state JT values are multiplied by 2 for the odd nucleus N^{13}.

form factor has not yet been derived.[14-17] Consequently we adopt here the so-called well-depth or separation energy procedure which gives the neutron form factor the proper asymptotic behavior by increasing the well depth to accommodate increasing separation energy. This means that before transfer the neutrons are in a potential well, with a single-particle binding energy E_B, given by

$$E_B = \tfrac{1}{2}[S_{nn} + E^*], \tag{1}$$

where S_{nn} is the two-neutron separation energy between ground states and E^* is the excitation energy of the final state. Since E^* can be as much as 15 MeV, this commonly used recipe for E_B produces a large attenuation in the form factors and hence in the cross sections for highly excited states. Although cross sections calculated in this way represent experiment fairly well, the procedure seems difficult to justify. Some comments on this point will be made in the discussion. One consequence is that the calculations are quite insensitive to whether the $1p_{3/2}$ and $1p_{1/2}$ levels are separated by several MeV or degenerate, since the neutrons are so tightly bound.

For the bound-state well a radius $R = 1.25A^{1/3}$ fm

TABLE III. Relative transition strengths for $N^{15}(p,t)$ to four final states in N^{13} when the separation-energy technique is used and when the neutron binding energies are kept fixed from state to state.

N^{13} final state (JT)		Separation energy $(S_{nn}+E^*)$	Transition strengths		
			Exptl.	$\epsilon_{p3/2}=\epsilon_{p1/2}=-\frac{1}{2}S$	$\epsilon_{p3/2}=-10.0$ MeV $\epsilon_{p1/2}=-3.5$ MeV
$\frac{1}{2}$	$\frac{1}{2}$	21.388	1	1	1
$\frac{3}{2}$	$\frac{1}{2}$	24.898	0.55	0.68	0.73
$\frac{5}{2}$	$\frac{1}{2}$	28.768	0.90	1.91	3.43
$\frac{3}{2}$	$\frac{3}{2}$	36.458	0.076	0.16	0.87

and a diffusivity $a = 0.65$ fm were used. A constant radius for all wells throughout the $1p$ shell was obtained by setting $A = 15$ in all relations $R = r_0 A^{1/3}$.

Table III contains a comparison of the relative transition strengths to the four final states of N^{13} for the situations when either a constant neutron binding energy or the separation technique are used. Potential S is used in this comparison, and the states are normalized to the ground-state strength. Here, as elsewhere in this work, the integral of the cross section from c.m. angles $\theta = 15$ to $50°$, i.e., $\int_{15}^{50} (d\sigma/d\Omega) d\Omega$, is used as a measure of transition strength. The integral covers the second peak for $L = 0$ transfer and the first peak for $L = 2$ transfer. Unfortunately very little data exist for smaller angles, so that not much is known about the primary $L = 0$ peak. It is apparent that for the N^{15} target, the separation energy technique is vastly to be preferred. This conclusion obtains whether we use potentials S or V and independently of the target nucleus. For our standard transitions $N^{15}(p,t)N^{13}$, the angular distributions are displayed in Fig. 2. The quality of fit is very good for triton potential S but deteriorates somewhat in the $L = 2$ transfers for potential V.

With the triton optical potentials selected, it is possible to systematically present the fits to transitions throughout the $1p$ shell. This is done for the angular distributions in Figs. 3 through 5. Figure 3 collects together purely or dominantly, low-lying $L = 0$ transitions, and Fig. 4 some purely or dominantly $L = 2$ transfers. Figure 5 contains two distributions for transitions to analog states and one in which $L = 0$ and $L = 2$ transfers mix. Figure 6 displays graphically a comprehensive comparison with experiment of the transition strengths obtained using both potentials S and V. The experimental magnitudes are given in the fifth column of Table I, and the O^{16}-O^{14} ground-state transition in this latter table is used to normalize all calculated strengths. The normalization constants (i.e., the numbers by which one must multiply the calculated cross sections to obtain the experimental magnitudes) are 7.73 and 2.05 for the triton potentials S and V, respectively. The degree of similarity between experimental and calculated strengths is quite encouraging, although not so good as was the case in single-particle transfer. However, taking into account the extra sensitivity inherent in the two-particle process, there is a fair correlation in the relative magnitudes for calculated and observed transitions.

One can make some other statements about the fits. First, we have implied that it was important to keep nuclear radii constant when potential S is used. Figure 7 shows a comparison with experiment of angular distributions obtained with and without an $A^{1/3}$ radius dependence for a particularly sensitive $L = 0$ transition C^{12} to the ground state of C^{10}. This same situation obtains for the equally high negative-Q transition $C^{13} \rightarrow 33$ shown in Fig. 5.

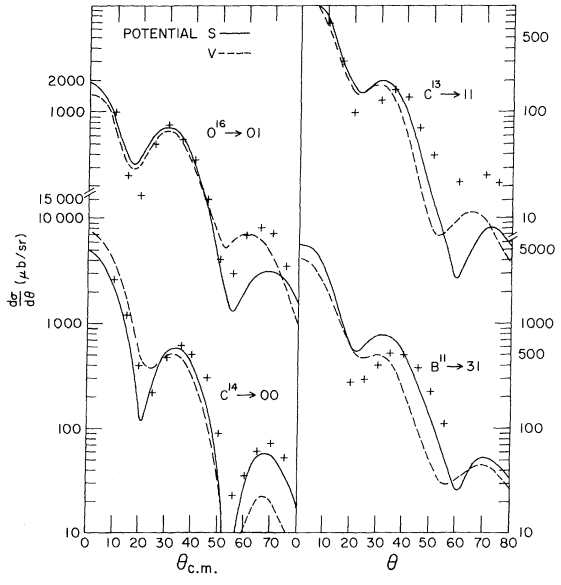

FIG. 3. Comparison with experiment for some purely or dominantly $L = 0$ transitions. Final-state JT values are listed as such for even nuclei and multiplied by 2 for odd nuclei.

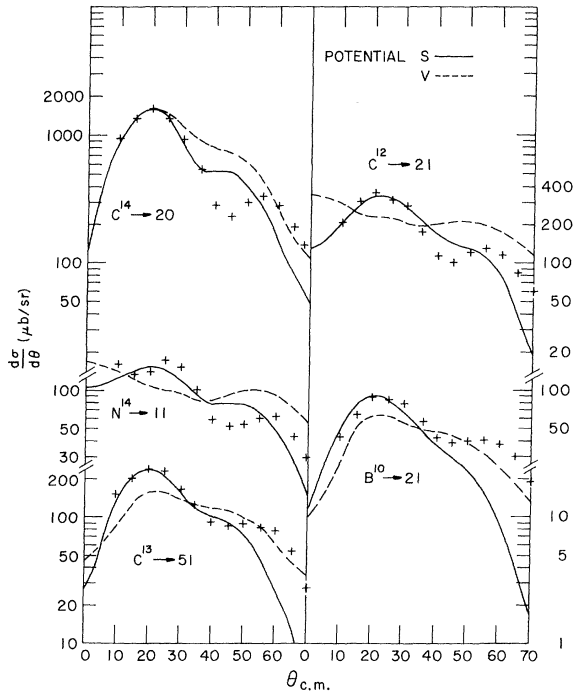

FIG. 4. Comparison with experiment for some purely or dominantly $L = 2$ transitions.

From the latter figure it is also evident that triton potential V gives a superior description of some large Q transitions. In general the angular distributions obtained with V are less sensitive to radius variations. Also there is a failure of either triton optical potential to fit angular distributions throughout the considered mass region. This is probably a consequence of having kept the potential parameters constant. Another characteristic failing of many potential S angular distributions is a too rapid drop-off in cross section with increasing angle. This difficulty is mitigated to some extent when the triton potential V is used.

Spin-orbit forces have to this point been ignored in both the continuum and bound-state wells. As noted earlier, any departure from the equal division of the separation energy between the transferred neutrons to account for a $p_{3/2}$-$p_{1/2}$ splitting was not significant. Reasonable spin-orbit forces in the proton and triton channels led to a very slight increase in cross sections at angles 50 to 70° and , of course, a larger increase at more backward angles.

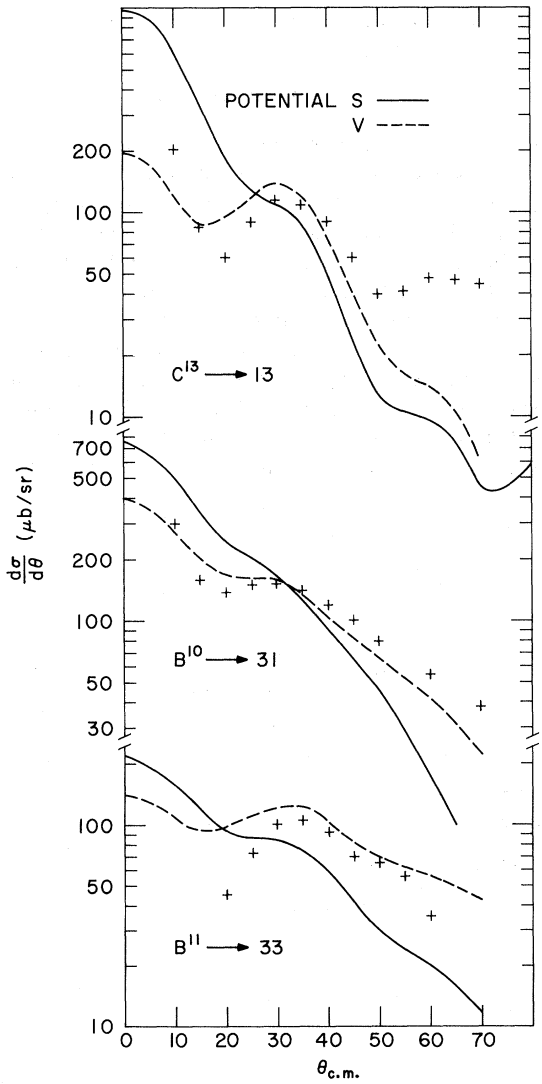

FIG. 5. Comparison with experiment for two transitions to analog states ($C^{12} \rightarrow 13$ and $B^{11} \rightarrow 33$) and for one transition $B^{10} \rightarrow 31$ in which $L=0$ and $L=2$ transfer are nontrivially mixed.

III. DISCUSSION

A. DWBA Analysis

First it is evident that the theory of the two-nucleon-transfer form factor is in a very primitive state. We have in this work taken an easy way out by fixing on a specific prescription, the separation-energy technique. Only an *ad hoc* justification can be given for this approach; it would otherwise have been difficult to obtain the observed falloff of transition strength with increased separation energy. In the ($N^{15} \rightarrow N^{13}$) transitions, for example, this conclusion can be reached by examining only the $L=2$ transitions. Also, in $L=0$ pickup from C^{13}, the nuclear-structure factors indicate a ratio of almost 7 in cross-section favoring transition to the $(\frac{1}{2}, \frac{3}{2})$ analog state at 12.45 MeV in C^{11} over transition to the $(\frac{1}{2}, \frac{1}{2})$ state at 2.00 MeV. However, the much greater value of E_B for the analog transition produces cross sections that are nearly equal in the DWBA calculation with surface absorption for tritons. While it is true that the form factor is treated correctly asymptotically by this energy procedure, it is equally true that inner regions of the nucleus are sampled in the reaction. In Table IV are displayed the changes in magnitude obtained in the transitions from N^{15} to the ground and analog states in N^{13}, when a lower cutoff is placed on

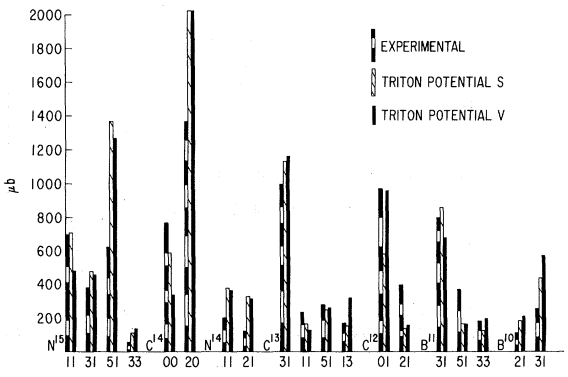

FIG. 6. A comprehensive graphical comparison of calculated and experimental transition strengths for both triton potentials S and V. The measure of strength is the integrated cross section between c.m. 15 and 50° except for the B^{11} transitions where the interval 20 to 55° is used.

the triton orbital angular momentum. Since appreciable changes in cross section occur when low angular momenta are removed, fairly small radii near the nuclear surface must be involved. We have quoted in Table IV a radius within which 75% of the cross section occurs. This radius is obtained using the simple relation $m_t v_t r = l\hbar$. It is rather interesting that similar radii calculated for the much smaller Q transitions in $C^{14}(p,t)C^{12}$ are some 1.5 to 2 times as large. Calculations have been published which include an approximate factor for the effect of finite range and also including nonlocal optical potentials.[18] These seem to improve the calculated magnitudes of states at high excitation relative to those at lower excitation.

One of the simplifying features employed in the calculation of a two-particle form factor[14,15] was a replacement of the neutron-proton force $v(\vec{r}_1 - \vec{r}_p) + v(\vec{r}_2 - \vec{r}_p)$ by the pseudoforce $\delta[r_p - \frac{1}{2}(\vec{r}_1 + \vec{r}_2)]$. Not only is the force made zero range in some sense, but only a dependence on the separation between proton and the two-neutron c.m. is retained. If a finite-range force or even a more normal zero-range force $\delta(\vec{r}_1 - \vec{r}_p) + \delta(\vec{r}_2 - \vec{r}_p)$ is used, some modification in the form factor will result. One of the striking features of the experimental data was the apparent existence of a universal shape for the $1p$-shell angular distributions, especially for $L=0$ transfer. For some transitions it was difficult to reproduce such a shape with the codes at hand; especially bad were the shapes obtained for the high negative-Q transitions from C^{13} and C^{12} targets. Perhaps a finite-range calculation would improve these shapes.

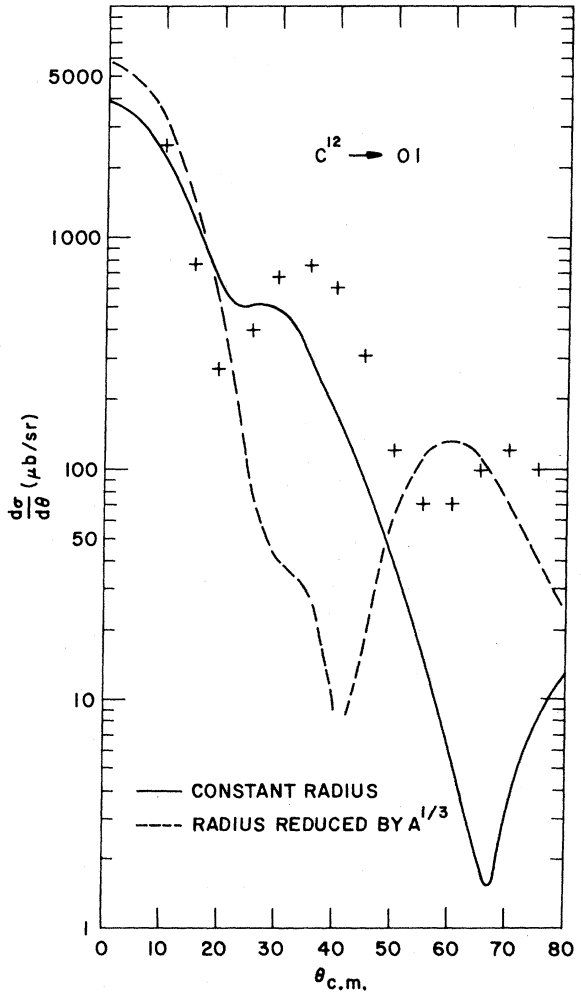

FIG. 7. Some evidence for using constant radii throughout the $1p$ shell in optical and bound-state wells. Two angular distributions are shown for the transitions $C^{12} \rightarrow 01$, one in which radii have been kept the same as in $N^{15}(p,t)N^{13}$ or one in which all radii have been reduced by the usual $A^{1/3}$ dependence.

B. Effect of $(2s, 1d)$ Admixture

The calculated cross sections are based on pure $1p$-shell wave functions. One objective of our survey was to see whether the nature of the disagreements with experiment suggests the expected presence of $(2s, 1d)$ admixtures in the wave functions. It has been emphasized[16] that such admixtures have little effect on the angular distributions, so that one must consider the magnitudes of the cross sections. Furthermore, since we have used a normalization to the $L=0$ transfer from O^{16} observable $(2s, 1d)$ effects must differ from those present in that transition. The outstanding difference in the

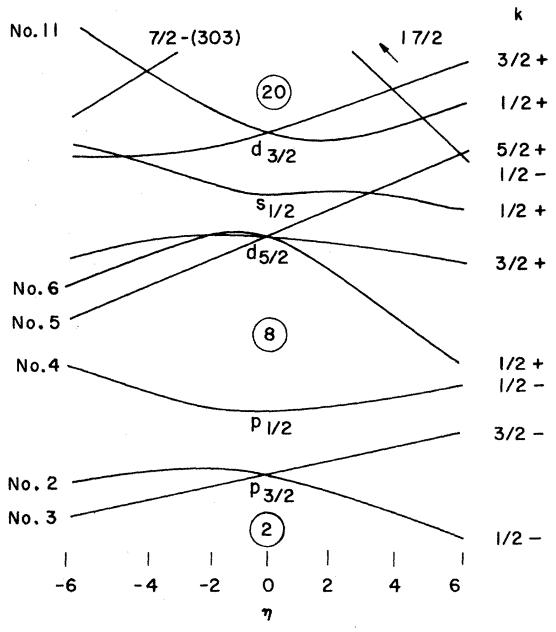

FIG. 8. The Nilsson-level scheme for nucleon numbers 2 to 20.

TABLE IV. Relative transition strengths for the two reactions (1) $N^{15}\rightarrow$ the ground state in N^{13} ($L=0$) and (2) $N^{15}\rightarrow$ analog state in N^{13} ($L=2$), when a lower cutoff (l_{min}) is placed on the triton orbital angular momentum. A radius $r_{75\%}$, inside of which 75% of the cross section occurs, is also shown.

l_{min}	Relative magnitudes $N^{15}\rightarrow \frac{1}{2}\frac{1}{2}$ $(L=0)$	$N^{15}\rightarrow \frac{3}{2}\frac{3}{2}$ $(L=2)$
0	1	1
2	0.61	0.76
4	0.40	0.41
6	0.19	0.20
8	0.04	0.03
10	0.002	0.0001
$r_{75\%}$	2.8 fm	4.1 fm

strong transitions is that the calculated magnitudes for C^{14} to the (2, 0) state of C^{12} and for N^{15} to the $(\frac{5}{2}, \frac{1}{2})$ state of N^{13} are much larger than observed. There is an interesting qualitative explanation of these differences in terms of $(2s, 1d)$ admixtures.

A useful representation for treating this problem is obtained from many-particle intrinsic states formed by putting nucleons into the deformed orbitals of Nilsson model[19] shown in Fig. 8. The intrinsic state for the first two levels of C^{12} is formed by filling the two lowest $1p$ orbitals No. 2, No. 3 for oblate deformation $\eta\approx -6$. The intrinsic state for C^{14} is found by adding two neutrons in the uppermost $1p$ orbital No. 4. It has been shown[20] that angular momentum eigenfunctions projected from these intrinsic states are very similar to the lowest states resulting from diagonalizing a two-body interaction within the $1p$ shell.

From Fig. 8 one sees that there are several positive-parity levels from the $(2s, 1d)$ shell near the uppermost $1p$ orbital for oblate deformation. It seems reasonable that the neutron pair might be partially in the positive-parity orbitals although predominantly in the $1p$ orbital. The simplest procedure is to assume an attractive pairing interaction to calculate this admixture and obtain the resultant two-nucleon c.f.p.'s for $(2s, 1d)$ pickup from C^{14}. The case of $N^{15}(p,t)N^{13}$ $(T=\frac{1}{2})$ can be calculated in the same way with an odd proton standing by as spectator in the uppermost $1p$ orbital.

In order to obtain the qualitative effective we have carried out a simplified calculation for $\eta=-6$, including the $k=\frac{1}{2}^-$ level No. 4 and only two positive-parity levels, Nos. 5 and 6, neglecting the difference in energy of the two positive-parity levels. There is then just one parameter, the ratio, ϵ, of the pairing-interaction strength to the separation of positive- and negative-parity orbitals. If we choose $\epsilon=0.5$, the intensities of the components of the two-neutron intrinsic state are

$$90\%\ (k=\tfrac{1}{2}^-)^2,\quad 5\%\ (k=\tfrac{5}{2}^+)^2,$$

and

$$5\%\ (k=\tfrac{1}{2}^+)^2.$$

The resulting two-particle c.f.p.'s are presented in Table V using phases consistent with the Bayman convention in TWO PAR. One should note that Nilsson uses a $2s$ radial wave function different in sign. For comparison the original $1p$-shell c.f.p.'s are also shown as are those obtained from level No. 4 by itself. There is clearly a close correspondence between the full spherical shell model and the projected-rotational model.

As one might expect, the $L=0$ transition strength is increased by the pairing calculation. Rather surprisingly the $L=2$ transition is suppressed.

TABLE V. Two-particle c.f.p.'s appropriate to the $L=0,2$ transitions $C^{14}(p,t)C^{12}$ for the cases: (1) $1p$-shell model, (2) a projected rotational model including only the Nilsson orbital No. 4, and (3) a projected rotational-plus-pairing model involving levels No. 4, No. 5, and No. 6. The phases used are those appropriate to the Bayman code TWO-PAR, for which the radial wave functions are all positive near the origin.

	Two-particle c.f.p.'s					
			Projected-rotational		Projected-rotational and pairing	
	$1p$-shell model		Level No. 4		Levels No. 4, No. 5, No. 6	
Configuration	$L=0$	$L=2$	$L=0$	$L=2$	$L=0$	$L=2$
$1p_{3/2}{}^2$	−0.067	0.078	−0.056	0.083	−0.053	0.079
$1p_{1/2}{}^2$	−0.105		−0.115		−0.108	
$1p_{3/2}\,1p_{1/2}$		0.195		0.198		0.188
$2s_{1/2}{}^2$					0.027	
$1d_{5/2}-2s_{1/2}$						0.041
$1d_{5/2}{}^2$					0.033	0.036
$1d_{3/2}{}^2$					0.002	−0.002
$1d_{3/2}-2s_{1/2}$						−0.016
$1d_{5/2}-1d_{3/2}$						−0.002

TABLE VI. The transition strength obtained using the c.f.p.'s of Table V, compared with experimental values.

	Strengths $L=0$	Strengths $L=2$	Ratio $L=0/L=2$
Experiment	768μb	1362	0.564
$1p$-shell model	585	2032	0.288
Projected-rotational and pairing	568	2151	0.264
Projected-rotational and pairing			0.684
(a) No. 4, No. 5, No. 6	793	1158	0.684
(b) No. 4, No. 5, No. 11	684	2641	0.259

The reason for the opposite effect in $L=0$ and $L=2$ transfer lies in the nature of the Nilsson orbitals. From Fig. 8 we see that in an oblate field, the low positive-parity orbitals go to lower energy with increasing deformation while the uppermost $1p$ orbital is rising. This is because the low positive-parity orbitals are oblate, while the $1p$ orbital is prolate. The admixed two-neutron state is therefore less prolate than if it were made with $1p$ orbitals, so while the pairing interaction increases its $L=0$ component, it reduces the $L=2$ component. Indeed, if the prolate level No. 11 is substituted in the calculation for No. 6, an enhancement of the $L=2$ strength results. In Table VI are displayed the cross sections deduced from the pairing calculation and the resulting enhancement in the $L=0$ to $L=2$ ratio. Also quoted are the results obtained when the substitution No. 6 $\rightleftharpoons$ No. 11 is made. Detailed analysis indicates that the dominant components in the transfer reaction are those involving the more spatially extended $2s$ orbit. Removing the $(d_{5/2}{}^2)$ mixtures in either the $L=0$ or $L=2$ transfer affects the cross sections by ~10%. It is the change in sign of the $(2s\text{-}1d)$ components in the case where level No. 11 replaces level No. 6, which converts the suppression of the $L=2$ transfer into an enhancement.

The relative effects on $L=0$ and $L=2$ transfer therefore depend on the type of orbitals being mixed. In our $1p$-shell cases we would expect, according to Fig. 8, that for targets C^{13} and lower A, $(2s, 1d)$ admixture would enhance both $L=0$ and $L=2$ transfer, since the neutrons lie in $1p$ orbitals having the same shape as the lower positive-parity orbitals. However, near the closing of a major shell it should be generally true that the admixture of nearby opposite parity states suppresses $L=2$ transfer and enhances $L=0$ transfer.

A spherical model which also approximates the above situation is obtained by initially representing C^{14} by the configuration $[p_{3/2}{}^4]^0$. This fiction of equating $p_{1/2}$ and $p_{3/2}$ orbitals allows one to simply include both $L=0$ and $L=2$ pairs in the ground state. The final state in C^{12} to which transitions occur are taken as $(p_{3/2}{}^2)^{0,2}$. A short-range attractive force will admix the configurations $[(p_{3/2}{}^2)^0(d_{5/2}{}^2)^0]^0$, $[(p_{3/2}{}^2)^0, (d_{5/2}{}^2)^0]^0$ and somewhat more weakly the configurations $[(p_{3/2}{}^2)^2, (d_{5/2}{}^2)^2]^0$, $[(p_{3/2}{}^2)^2, (d_{5/2}s_{1/2})^2]^0$ into the C^{14} ground state. Since the two-particle c.f.p.'s for the $L=0, 2$ transitions are initially -0.15, 0.33, i.e., larger for an $L=2$ transfer, the final result is a preferential enhancement of the $L=0$ strength. However, this latter enhancement mechanism is not nearly so efficient as the previously described rotational model.

IV. CONCLUSIONS

The attempt to correlate experiment and calculations for a large number of (p,t) transitions in different $1p$-shell nuclei has been reasonably successful. An over-all similarity to experiment in the calculated shapes and magnitudes has been achieved. Probably some improvement would obtain if either potential S or V were allowed to vary with mass number and with triton energy. Nevertheless, the use of average or at least smoothly varying optical parameters was crucial for relating the magnitudes of the many transitions. The over-all factor of approximately 4 between the cross sections deduced from our two triton potentials demonstrates the danger inherent in using too different an optical potential for each nucleus. The approximations used are undoubtedly not as reliable in the treatment of transitions to highly-excited analog states. This feature together with the experimental observation that cross sections to such states are generally weaker than expected, means that the study of analog spectra is, unfortunately, relatively difficult. Despite this the calculations give a good first-order representation of observation for the analog states.

The degree of discrepancy between calculation and observation precludes making quantitative estimates of the effect of $(2s, 1d)$ admixtures. However, we do believe the comparison gives qualitative evidence for the presence of such admixture in the C^{14} and N^{15} ground states, admixtures which enhance the $L=0$ cross sections and suppress the $L=2$ cross sections. This feature can be produced by means of a deformed representation, as we have done in Sec. III, and thus help to alleviate the major discrepancies with the data in strong transitions.

Some interest must eventually be focused on deducing absolute cross sections from the DWBA analysis. This point is underscored by the large difference in cross sections obtained with the tri-

ton potentials S and V. Unfortunately, this cannot be done without refining the treatment of the transfer reaction. In particular, one must include a finite-range force and also provide a more satisfying means of joining up the asymptotic to the small radius behavior of the form factor.[17] It remains to be seen whether such evolutions of the theory will provide a much better agreement with observation, both in magnitudes and shapes of cross sections. It has been noted previously that spin-dependent features should be included. Recent experiments with polarized protons[21] indicate that the asymmetries for some transitions are not reproduced by DWBA calculations.

Nothing has been said here about the experimental accuracy of the cross sections; this accuracy is probably much better than that of the DWBA analysis. However, there are some points which need clarification. For example, differences do exist between the $N^{14}(p,t)$ and $N^{14}(p,He^3)$ transitions[5,18] to the pairs of analog states (1, 1) and (2, 1). The ratio of magnitudes, $\sigma(11)$ to $\sigma(21)$, is 1.70 for (p,t) and 1.25 for (p,He^3). Furthermore, at forward angles the cross section $\sigma(11)$ appears to rise in the (p,t) reaction, but drop in the (p,He^3) reaction. This is a potentially important feature; the $1p$ calculation predicts a negligible $L=0$ component in this mixed $L=0,2$ transition. Hence this would be a place to detect an $L=0$ $(2s\text{-}1d)$ component. The point we wish to emphasize is the desirability of having data at as small angles as is experimentally feasible in cases where $L=0$ transfer is allowed.

V. ACKNOWLEDGMENT

We wish to once again thank B. F. Bayman and P. D. Kunz for their DWBA codes. We are also indebted to J. C. Hardy, J. M. Loiseaux, G. T. Garvey, C. C. Maples, J. Cerny, D. G. Fleming, D. K. Olsen, and R. E. Brown for the use of experimental data before publication. One of us (D.K.) wishes to thank Brookhaven National Laboratory for its hospitality.

---

*Work performed under the auspices of U. S. Atomic Energy Commission.

†Permanent address: Physics Department, Argonne National Laboratory, Argonne, Illinois.

[1]J. P. Schiffer, G. C. Morrison, R. H. Siemssen, and B. Zeidman, Phys. Rev. 164, 1274 (1967).

[2]S. Cohen and D. Kurath, Nucl. Phys. A141, 145 (1970).

[3]J. Cerny and R. H. Pehl, Phys. Rev. Letters 12, 619 (1964).

[4]D. G. Fleming, J. Cerny, C. C. Maples, and N. K. Glendenning, Phys. Rev. 166, 1012 (1968).

[5]C. C. Maples, J. Cerny, and D. G. Fleming, private communication.

[6]D. K. Olsen and R. E. Brown, John H. Williams Laboratory, University of Minnesota, Annual Report, 1970 (unpublished).

[7]D. G. Fleming, J. Cerny, and N. K. Glendenning, Phys. Rev. 165, 1153 (1968).

[8]S. W. Cosper, R. L. McGrath, J. Cerny, C. C. Maples, G. W. Goth, and D. G. Fleming, Phys. Rev. 176, 1113 (1968).

[9]S. W. Cosper, H. Brunnader, J. Cerny, and R. L. McGrath, Phys. Letters 25B, 324 (1967).

[10]J. C. Hardy, J. M. Loiseaux, J. Cerny, and G. T. Garvey, to be published.

[11]G. T. A. Squier, A. R. Johnston, E. W. Spiers, S. A. Harbison, and N. M. Stewart, Nucl. Phys. A141, 158 (1970).

[12]D. Armstrong, J. Blery, P. Keaton, Jr., and L. Veeser, Los Alamos Scientific Laboratory Report No. LA-4177 (unpublished).

[13]H. T. Fortune, N. G. Puttaswamy, and J. L. Yntema, Phys. Rev. 185, 1546 (1969).

[14]N. K. Glendenning, Phys. Rev. 137, B102 (1965).

[15]B. F. Bayman and A. Kallio, Phys. Rev. 156, 1121 (1967).

[16]R. L. Jaffe and W. J. Gerace, Nucl. Phys. A125, 1 (1969).

[17]R. H. Ibarra and B. F. Bayman, Phys. Rev. C 1, 1786 (1970).

[18]D. K. Scott, P. M. Portner, J. M. Nelson, A. C. Shotter, A. J. Mitchell, N. S. Chant, D. G. Montague, and K. Ramavatoram, Nucl. Phys. A141, 497 (1960).

[19]B. R. Mottelson and S. G. Nilsson, Kgl. Danske Videnskab. Selskab, Mat.-Fys. Medd. 1, No. 8 (1959).

[20]D. Kurath and L. Picman, Nucl. Phys. 10, 313 (1959).

[21]J. C. Hardy, A. D. Bachy, G. R. Plattner, J. A. Macdonald, and R. G. Sextro, University of California Radiation Laboratory Report No. UCRL-19912 (unpublished).